CRYSTAL GROWTH & DESIGN
2007
VOL. 7, NO. 10
1992−1998

Metal-Directed Supramolecular Architectures: From Mononuclear to 3D Frameworks Based on In Situ Tetrazole Ligand Synthesis

Zhen Li,[†] Mian Li,[†] Xiao-Ping Zhou,[†] Tao Wu,[†] Dan Li,*[,†] and Seik Weng Ng[‡]

Departments of Chemistry, Shantou University, Guangdong 515063, People's Republic of China, and University of Malaya, 50603 Kuala Lumpur, Malaysia

Received March 10, 2007; Revised Manuscript Received July 10, 2007

ABSTRACT: This work focuses on the investigation of the influence of metal ions and supramolecular interactions on the self-assembly of in situ generated tetrazolate coordination architectures. A series of new metal−organic complexes, $[Zn(pzta)_2(H_2O)_2]$ (**1**), $[Cu(pzta)_2](H_2O)_3$ (**2**), $[Cd(pzta)_2]_n$ (**3**), $[Ag(pzta)]_n$ (**4**), and $[Cd_2(pzta)(OH)(SO_4)]_n$ (**5**) [pzta = pyrazinyl tetrazolate], have been achieved by the in situ hydrothermal reactions of pyrazinecarbonitrile, sodium azide, and different metal ions. Complexes **1** and **2** have similar mononuclear structures bearing distinct intermolecular hydrogen-bond interactions to form two different 3D supramolecular networks based on 4^4-subnets. Complex **3** features a 1D crossed-shape chain structure. Complex **4** is a coordination polymer comprised of mildly undulated 2D layers with a (4.8^2) topological network. Complex **5** is a 3D diamondoid framework constructed by pentanuclear cadmium cluster nodes and pzta linkers. The configurations of complexes **1**−**5** span from mononuclear (**1**, **2**), to one-dimensional (**3**) and two-dimensional (**4**), to three-dimensional (**5**), which indicates that metal ions play an essential role in the framework formation of the in situ generated tetrazolate architectures. Furthermore, complexes **1**, **3**, and **5** exhibit strong blue photoluminescence in similar energy regions.

Introduction

From the viewpoint of crystal engineering, the intrinsic geometric preferences of metal centers and various coordination sites of bridging ligands are the pivotal factors in determining the supramolecular architectures. Recently, it appears from the literature that metal-directed self-assembly is one of the most useful strategies for generating intriguing metallosupramolecular architectures,[1] because it not only has the advantage in rational bottom-up construction for its regulated coordination geometry, but also plays an important role in influencing the molecular architectures with unique properties.[2−6] Some remarkable examples of the metal-directed approach have been documented in recent years, including metal-directed assembly of molecular loop and tetrahedron,[2] metal-directed macrocycle expansion,[3] metal-assisted ligand-centered redox potential,[4] metal-regulated mixed-ligand metal−organic frameworks,[5] and metal-directed stereoselective syntheses of homochiral complexes,[6] and so forth.

On the other hand, due to the diversity of the connecting modes and the high structural stability, the polydentate N donor ligands have been employed extensively as chelating or bridging linkers.[7] Tetrazolate-based ligands have been shown to be excellent and versatile building blocks, forming a great variety of supramolecular entities possessing an interesting chemical rearrangement reaction[8a] and magnetic[8b] and optical properties.[9,11,12] Recently, Sharpless et al. reported the click chemistry for the synthesis of a variety of tetrazoles through [2 + 3] cycloaddition reactions of nitriles and azide in the presence of zinc salt as Lewis acid.[10] This synthetic approach has been extended by varying metal ions such as Zn(II),[9a−e] Cd(II),[9e−g] Cu(I)/Cu(II),[11a−b,12] and Ag(I)[9h,11c,12] in the construction of coordination frameworks.

In our continuing research on the crystal engineering of metal tetrazolate complexes,[11] we reported herein a series of metal-directed tetrazolate coordination frameworks with various dimensions containing in situ generated pryzinyl tetrazole (pzta) ligand. Besides the utilization of the metal-directed approach for building diverse coordination geometries such as square-planar, octahedral, and so on, we also take into account the effect of hydrogen bonds and other supramolecular interactions for extending architecture dimensionality.[13] As shown in Scheme 1, five new complexes, $[Zn(pzta)_2(H_2O)_2]$ (**1**), $[Cu(pzta)_2](H_2O)_3$ (**2**), $[Cd(pzta)_2]_n$(**3**), $[Ag(pzta)]_n$ (**4**), and $[Cd_2(pzta)(OH)(SO_4)]_n$ (**5**), have been synthesized and characterized. The configurations of **1**−**5** exhibit an increasing dimensionality spanning from mononuclear (**1**−**2**), to one-dimensional (**3**) and two-dimensional (**4**), to three-dimensional (**5**).

Scheme 1. In Situ Hydrothermal Syntheses of Complexes 1−5

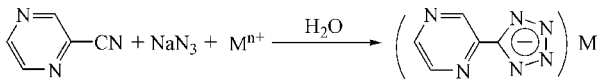

M^{n+} = Zn(II), Cu(II), Cd(II), Ag(I)

Experimental Section

Materials and Physical Measurements. All chemicals were obtained from commercial sources and used as received. Infrared spectra were obtained in KBr disks on a Nicolet Avatar 360 FTIR spectrometer in the range 4000−400 cm^{-1}. Elemental analyses were determined with a Perkin-Elmer 2400C elemental analyzer. Photoluminescence measurements were carried out using crystalline samples, and the spectra were collected with a Perkin-Elmer LS 55 spectrofluorimeter.

Syntheses. $[Zn(pzta)_2(H_2O)_2]$ (1). A mixture of $ZnCl_2$ (0.0273 g, 0.20 mmol), NaN_3 (0.0130 g, 0.20 mmol), and pyrazinecarbonitrile (pzCN) (0.0105 g, 0.10 mmol) was sealed in a 15-mL Teflon-lined stainless steel reactor. Water (6.0 mL) was added to the reactor and then stirred for 10 min in air. The reactor was heated in an oven at 140 °C for 72 h and then cooled to room temperature at a rate of 5 °C·h^{-1}. Colorless blocklike crystals were collected and dried in air (yield 60% based on pzCN). IR (KBr pellet, cm^{-1}): 3347s, 3081s, 2067w, 1978w, 1857w, 1799w, 1635m, 1533w, 1465w, 1417s, 1372s, 1358s, 1295w, 1225m, 1136s, 1039s, 938w, 864s, 757m. Anal. Calcd (%) for $C_{10}H_{10}N_{12}O_2Zn$ (395.67): C, 30.36; H, 2.55; N, 42.48. Found (%): C, 30.12; H, 2.83; N, 42.74.

$[Cu(pzta)_2](H_2O)_3$ (2). Complex **2** was prepared using the method similar to that for complex **1** except that $ZnCl_2$ was replaced by Cu-

[†] Shantou University.
[‡] University of Malaya.

10.1021/cg0702333 CCC: $37.00
Published on Web 09/05/2007

Table 1. Summary of the Crystal Data and Structure Refinement Parameters for 1−5

	1	2	3	4	5
formula	$C_{10}H_{10}N_{12}O_2Zn$	$C_{10}H_{12}CuN_{12}O_3$	$C_{10}H_6CdN_{12}$	$C_5H_3AgN_6$	$C_5H_4Cd_2N_6O_5S$
M_r	395.67	411.86	406.67	255.00	485.00
cryst syst	monoclinic	monoclinic	monoclinic	monoclinic	monoclinic
space group	$P2_1/n$	$C2/c$	$P2_1$	$P2_1/c$	$C2/c$
a/Å	6.0910(6)	13.0083(10)	8.7615(6)	3.5465(6)	20.1345(5)
b/Å	11.4576(12)	7.3160(6)	18.5982(13)	12.373(2)	10.5451(3)
c/Å	10.6860(11)	16.8582(13)	9.0395(6)	14.679(3)	13.3534(3)
α/deg	90	90	90	90	90
β/deg	105.626(2)	101.9220(10)	105.5030(10)	92.638(3)	131.39
γ/deg	90	90	90	90	90
Z	2	4	4	4	8
V (Å^3)	718.188	1569.755	1419.387	643.443	2127.060
D_c/g cm^{-3}	1.830	1.743	1.903	2.632	3.029
μ/mm^{-1}	1.749	1.436	1.560	3.069	4.224
reflns collected	4470	4699	9576	4156	8513
unique reflns	1629	1791	5516	1559	2399
R_{int}	0.0207	0.0204	0.0179	0.0146	0.0235
GOF	1.051	1.129	1.058	1.083	1.082
R1 [$I > 2\sigma(I)$][a]	0.0311	0.0414	0.0291	0.0292	0.0233
wR2 [$I > 2\sigma(I)$][b]	0.0774	0.1113	0.0769	0.0634	0.0588
R1 [all data]	0.0364	0.0450	0.0301	0.0338	0.0242
wR2 [all data]	0.0802	0.1135	0.0775	0.0652	0.0597

[a] $R1 = \Sigma(||F_o| - |F_c||)/\Sigma|F_o|$. [b] $wR2 = [\Sigma_w(F_o^2 - F_c^2)^2/\Sigma_w(F_o^2)^2]^{1/2}$.

$(NO_3)_2 \cdot 3H_2O$ (0.0241 g, 0.10mmol) and at 120 °C. Blue blocklike crystals were collected and dried in air (yield 40% based on pzCN). IR (KBr pellet, cm^{-1}): 3391m, 3099w, 1653w, 1558w, 1457w, 1431m, 1075w, 1180w, 1048m, 1014w, 525w. Anal. Calcd (%) for $C_{10}H_{12}N_{12}O_3Cu$ (411.86): C, 29.16; H, 2.94; N, 40.81. Found (%): C, 29.22; H, 2.71; N, 40.35.

$[Cd(pzta)_2]_n$ (3). A mixture of $CdSO_4 \cdot (8/3)H_2O$ (0.0512 g, 0.20 mmol), NaN_3 (0.0130 g, 0.20 mmol), and pzCN (0.0105 g, 0.10 mmol) was sealed in a 15-mL Teflon-lined stainless steel reactor. Water (6.0 mL) was added to the reactor and then stirred for 10 min in air. The reactor was heated in an oven to 160 °C for 72 h and then cooled to room temperature at a rate of 5 °C·h^{-1}. Pure colorless rod-shaped crystals were filtered and dried in air (yield 77% based on pzCN). IR (KBr pellet, cm^{-1}): 3461m, 2081w, 1635w, 1532w, 1456w, 1403s, 1367m, 1288w, 1177m, 1154s, 1068m, 1033s, 854w, 755w, 601w, 515w, 478w. Anal. Calcd (%) for $C_{10}H_6N_{12}Cd$ (406.67): C, 29.54; H, 2.48; N, 41.33. Found (%): C, 29.51; H, 2.51; N, 41.35.

$[Ag(pzta)]_n$ (4). Complex **4** was prepared using the method similar to that for complex **1** except that $ZnCl_2$ was replaced by $AgPF_6$ (0.0253 g, 0.10 mmol). Orange stick-shaped crystals were collected and dried in air (yield 70% based on pzCN). IR (KBr pellet, cm^{-1}): 3454m, 3076w, 1639w, 1532w 1458w, 1415m, 1401w, 1143m, 1028m, 863w. Anal. Calcd (%) for $C_5H_3N_6Ag$ (255.00): C, 23.55; H, 3.95; N, 32.96. Found (%): C, 23.19; H, 3.58; N, 32.75.

$[Cd_2(pzta)(OH)(SO_4)]_n$ (5). Complex **5** was prepared using the method similar to that for complex **3** with a larger amount of $CdSO_4 \cdot (8/3)H_2O$ (0.1539 g, 0.60 mmol). Pure yellow blocklike crystals were collected and dried in air (yield 80% based on pzCN). IR (KBr pellet, cm^{-1}): 3569m, 3103w, 2360w, 1465w, 1408m, 1373w, 1125s, 1088s, 1036s, 993m, 869w, 697m, 603m, 535w, 470w. Anal. Calcd (%) for $C_5H_4N_6O_5SCd_2$ (485.00): C, 12.38; H, 0.83; N, 17.33. Found (%): C, 12.42; H, 0.81; N, 17.56.

X-ray Crystallography. The crystal structures **1**−**5** (CCDC 653376−653380) were determined by single-crystal X-ray crystallography. Data collections were performed using a Bruker-AXS SMART CCD area detector diffractometer with Mo Kα radiation with an ω-scan mode ($\lambda = 0.71073$ Å). The structures were solved by direct methods and refined by full-matrix least-squares refinements based on F^2. Empirical absorption corrections were carried out utilizing the SADABS routine. All non-hydrogen atoms were anisotropically refined. Hydrogen atoms were added geometrically and refined with a riding model. Hydrogen atoms of water molecule of **1** and **2** were located from the different Fourier maps and refined isotropically with the O−H distances fixing on 0.85 Å. Structure solutions and refinements were performed with the SHELXL-97 package.[14] Crystal data and experimental details for the complexes are given in Table 1. Selected bond lengths and angles are given in Table 2. Corresponding hydrogen bonding data for **1** and **2** are listed in Table 3.

Results and Discussion

Syntheses. Hydrothermal reactions of pyrazinecarbonitrile (pzCN) and sodium azide in the presence of different metal salts resulted in various pyrazinyl tetrazolate coordination complexes. IR spectroscopic measurements were conducted to verify the absence of a peak in the 2200 cm^{-1} region in the corresponding spectra of the products, suggesting that the nitrile groups are no longer present. Simultaneously, the emergence of a peak at 1400−1500 cm^{-1} confirms the formation of the tetrazolate groups, in accordance with previous reports.[9] Single-crystal X-ray diffraction analysis indicates that the tetrazolate groups in the five compounds were all deprotonated to form tetrazolate monoanions. It is suggested that the Sharpless [2 + 3] tetrazole synthesis method works effectively in the in situ formation of metal tetrazolate complexes from the reactions of pzCN and sodium azide. Since different metal ions were introduced to the hydrothermal reactions, it is predictable that distinct coordinating intrinsic information is included in different in situ synthetic systems, which leads to the structural variation of complexes **1**−**5**. Additionally, the molar ratio of metal/pzCN also affects the final synthetic products in this work, which is illustrated by the increasing structural dimensionality from the 1D chain (**3**) to the 3D diamondoid framework (**5**) by the increasing molar ratio of Cd(II)/pzCN in the Cd(II)−tetrazole reactions.

Hydrogen-Bonded Supramolecular Architectures of $[Zn(pzta)_2(H_2O)_2]$ (1) and $[Cu(pzta)_2](H_2O)_3$ (2). Complexes **1** and **2** consist of similar $[M(pzta)_2]$ neutral mononuclear structures, crystallizing in centrosymmetric space group $P2_1/n$. The M(II) ion locates in the symmetry center and is chelated by two deprotonated pzta ligands adopting the trans configuration. Two pyrazine nitrogen atoms and two tetrazole nitrogen atoms from different pzta ligands build the equatorial plane around the M(II) ions [Zn−N(1) 2.11650(7) Å, Zn−N(5) 2.19661(7) Å for **1** (Figure 1a); Cu(1)−N(1) 1.98107(5) Å, Cu(1)−N(5) 2.04882(5) Å for **2** (Figure 1b)], accordingly creating two stable five-membered chelate rings (M−N−C_2−N). The mononuclear structures of **1** and **2** are similar to those of the analogous complexes {Zn[5-(2-pyridyl)-tetrazolato]$_2(H_2O)_2$},[9e] {Mn[5-(2-pyridyl)-tetrazolato]$_2(H_2O)_2$},[15] and {Cd[5-(pyrazin-2-yl)tetrazolato]$_2(H_2O)_2$}.[16] Although all these complexes possess similar bidentate chelating mononuclear structures, there

Table 2. Selected Bond Lengths (Å) and Angles (deg) for Complexes 1−5[a]

		Complex **1**			
Zn(1)−O(1WA)	2.1016(17)	Zn(1)−O(1W)	2.1016(17)	Zn(1)−N(1A)	2.1166(16)
Zn(1)−N(1)	2.1166(17)	Zn(1)−N(5A)	2.1965(16)	Zn(1)−N(5)	2.1965(16)
O(1WA)−Zn(1)−O(1W)	180.000(1)	O(1WA)−Zn(1)−N(1A)	87.65(7)	O(1W)−Zn(1)−N(1A)	92.35(7)
O(1WA)−Zn(1)−N(1)	92.35(7)	O(1W)−Zn(1)−N(1)	87.65(7)	N(1A)−Zn(1)−N(1)	180.0
O(1WA)−Zn(1)−N(5A)	89.88(6)	O(1W)−Zn(1)−N(5A)	90.12(6)	N(1A)−Zn(1)−N(5A)	78.52(6)
N(1)−Zn(1)−N(5A)	101.48(6)	O(1WA)−Zn(1)−N(5)	90.12(6)	O(1W)−Zn(1)−N(5)	89.88(6)
N(1A)−Zn(1)−N(5)	101.48(6)	N(1)−Zn(1)−N(5)	78.52(6)	N(5A)−Zn(1)−N(5)	180.0
		Complex **2**			
Cu(1)−N(1)	1.981(2)	Cu(1)−N(1A)	1.981(2)	Cu(1)−N(5A)	2.049(2)
Cu(1)−N(5)	2.049(2)				
N(1)−Cu(1)−N(1A)	180.0	N(1)−Cu(1)−N(5A)	98.86(9)	N(1A)−Cu(1)−N(1A)	81.14(9)
N(1)−Cu(1)−N(5)	81.14(9)	N(1A)−Cu(1)−N(5)	98.86(9)	N(5A)−Cu(1)−N(5)	180.0
		Complex **3**			
Cd(1)−N(1)	2.355(3)	Cd(1)−N(5)	2.380(3)	Cd(1)−N(7)	2.326(4)
Cd(1)−N(13)	2.328(4)	Cd(1)−N(17)	2.484(4)	Cd(1)−N(19)	2.290(4)
Cd(2)−N(10)	2.341(4)	Cd(2)−N(11)	2.418(4)	Cd(2)−N(14)	2.305(4)
Cd(2)−N(2A)	2.310(4)	Cd(2)−N(22A)	2.338(3)	Cd(2)−N(23A)	2.385(3)
N(19)−Cd(1)−N(7)	95.00(14)	N(19)−Cd(1)−N(13)	104.86(12)	N(7)−Cd(1)−N(13)	92.58(13)
N(19)−Cd(1)−N(1)	92.26(12)	N(7)−Cd(1)−N(1)	110.81(14)	N(13)−Cd(1)−N(1)	149.80(13)
N(19)−Cd(1)−N(5)	161.11(13)	N(7)−Cd(1)−N(5)	85.06(14)	N(13)−Cd(1)−N(5)	94.00(12)
N(1)−Cd(1)−N(5)	70.26(12)	N(19)−Cd(1)−N(17)	89.71(14)	N(7)−Cd(1)−N(17)	162.93(13)
N(13)−Cd(1)−N(17)	70.35(13)	N(1)−Cd(1)−N(17)	85.33(14)	N(5)−Cd(1)−N(17)	95.74(13)
N(14)−Cd(2)−N(2A)	90.15(15)	N(14)−Cd(2)−N(22A)	109.27(13)	N(2A)−Cd(2)−N(22A)	91.89(12)
N(14)−Cd(2)−N(10)	91.88(13)	N(2A)−Cd(2)−N(10)	107.07(13)	N(22A)−Cd(2)−N(10)	151.70(14)
N(14)−Cd(2)−N(23A)	86.12(13)	N(2A)−Cd(2)−N(23A)	159.62(14)	N(22A)−Cd(2)−N(23A)	70.61(12)
N(10)−Cd(2)−N(23A)	93.09(13)	N(14)−Cd(2)−N(11)	162.12(13)	N(2A)−Cd(2)−N(11)	93.15(16)
N(22A)−Cd(2)−N(11)	88.20(14)	N(10)−Cd(2)−N(11)	70.34(13)	N(23A)−Cd(2)−N(11)	96.53(13)
		Complex **4**			
Ag(1)−N(3)	2.244(2)	Ag(1)−N(1A)	2.318(2)	Ag(1)−N(6B)	2.370(3)
Ag(1)−N(5A)	2.473(2)				
N(3)−Ag(1)−N(1A)	137.68(9)	N(3)−Ag(1)−N(6B)	107.72(9)	N(1A)−Ag(1)−N(6B)	97.05(9)
N(3)−Ag(1)−N(5A)	102.33(8)	N(1A)−Ag(1)−N(5A)	72.76(8)	N(6B)−Ag(1)−N(5A)	143.66(9)
		Complex **5**			
Cd(1)−O(5)	2.2825(18)	Cd(1)−O(5A)	2.2825(18)	Cd(1)−N(1)	2.377(2)
Cd(1)−N(1A)	2.377(2)	Cd(1)−O(1)	2.4794(19)	Cd(1)−O(1)	2.4794(19)
Cd(2)−O(5B)	2.2348(18)	Cd(2)−O(5)	2.2348(18)	Cd(2)−N(2C)	2.279(2)
Cd(2)−N(2A)	2.279(2)	Cd(2)−O(2B)	2.3364(18)	Cd(2)−O(2)	2.3364(18)
Cd(3)−O(4E)	2.2102(12)	Cd(3)−O(3)	2.2535(19)	Cd(3)−O(5)	2.2879(18)
Cd(3)−N(5E)	2.355(2)	Cd(3)−O(1A)	2.3935(18)	Cd(3)−N(3C)	2.520(2)
O(5A)−Cd(1)−O(5)	149.19(9)	O(5)−Cd(1)−N(1)	115.08(7)	O(5A)−Cd(1)−N(1)	85.86(7)
O(5)−Cd(1)−N(1A)	85.86(7)	O(5A)−Cd(1)−N(1A)	115.08(7)	N(1)−Cd(1)−N(1A)	97.10(10)
O(5)−Cd(1)−O(1A)	69.12(6)	O(5A)−Cd(1)−O(1A)	87.24(6)	N(1)−Cd(1)−O(1A)	95.91(7)
N(1A)−Cd(1)−O(1A)	154.85(6)	O(5)−Cd(1)−O(1)	87.24(6)	O(5A)−Cd(1)−O(1)	69.12(6)
N(1)−Cd(1)−O(1)	154.85(6)	N(1A)−Cd(1)−O(1)	95.91(7)	O(1A)−Cd(1)−O(1)	80.83(10)
O(5B)−Cd(2)−O(5)	180.00(13)	O(5B)−Cd(2)−N(2C)	87.76(7)	O(5)−Cd(2)−N(2C)	92.24(7)
O(5B)−Cd(2)−N(2A)	92.24(7)	O(5)−Cd(2)−N(2A)	87.76(7)	N(2C)−Cd(2)−N(2A)	180.00(12)
O(5B)−Cd(2)−O(2B)	87.43(6)	O(5)−Cd(2)−O(2B)	92.57(6)	N(2C)−Cd(2)−O(2B)	82.96(7)
N(2A)−Cd(2)−O(2B)	97.04(7)	O(5B)−Cd(2)−O(2)	92.57(6)	O(5)−Cd(2)−O(2)	87.43(6)
N(2C)−Cd(2)−O(2)	97.04(7)	N(2A)−Cd(2)−O(2)	82.96(7)	O(2B)−Cd(2)−O(2)	180.00(12)
O(4D)−Cd(3)−O(3)	170.77(7)	O(4D)−Cd(3)−O(5)	93.05(7)	O(3)−Cd(3)−O(5)	91.39(7)
O(4D)−Cd(3)−N(5E)	95.17(7)	O(3)−Cd(3)−N(5E)	81.08(8)	O(5)−Cd(3)−N(5E)	170.80(7)
O(4D)−Cd(3)−O(1A)	91.94(7)	O(3)−Cd(3)−O(1A)	97.17(7)	O(5)−Cd(3)−O(1A)	70.59(6)
N(5E)−Cd(3)−O(1A)	104.94(7)	O(4D)−Cd(3)−N(3C)	90.80(8)	O(3)−Cd(3)−N(3C)	81.07(8)
O(5)−Cd(3)−N(3C)	90.45(7)	N(5E)−Cd(3)−N(3C)	93.57(7)	O(1A)−Cd(3)−N(3C)	160.95(7)

[a] Symmetry codes for **1**: A $-x+1, -y+1, -z+1$. For **2**: $-x+1/2, -y+1/2, -z+1$. For **3**: A $x-1, y, z$. For **4**: A $-x+2, y+1/2, -z+1/2$; B $-x+2, -y+1, -z$. For **5**: A $-x+1/2, y+0, -z+1/2$; B $-x, -y+1, -z$; C $x-1/2, -y+1, z-1/2$; D $x, -y+1/2, z-1/2$; E $x, y-1, z$.

Table 3. Hydrogen Bonds of Complexes 1 and 2[a]

D−H···A	*d*(D−H) (Å)	*d*(H···A) (Å)	*d*(D···A) (Å)	∠(D−H···A) (deg)
		Complex **1**		
O(1W)−H(1W2)···N(4B)	0.847(10)	1.908(11)	2.753(2)	176(3)
O(1W)−H(1W1)···N(2C)	0.840(10)	2.003(11)	2.831(3)	168(2)
		Complex **2**		
O(1W)−H(1W1)···N(3B)	0.85580(2)	1.98479(5)	2.840(3)	178
O(1W)−H(1W2)···N(4C)	0.85591(2)	2.06736(5)	2.910(3)	168
O(2W)−H(2W1)···O(1W)	0.86290(2)	2.15312(5)	2.858(2)	139

[a] Symmetry codes for **1**: B $-x+3/2, y+1/2, -z+3/2$; C $x-1, y, z$. For **2**: B $x+1/2, y+1/2, z$; C $-x+1/2, -y-1/2, -z+1$.

exist remarkable differences in the supramolecular interactions among them.

The water molecules and hydrogen bond make the significant difference between complexes **1** and **2**. In **1,** two water molecules coordinate to the Zn(II) ion at the equatorial axial positions [Zn−O1w 2.10153(7) Å], giving rise to the octahedral geometry of complex **1** (Figure 1a). In contrast, in **2**, two water molecules locate at the equatorial axial positions of the Cu(II)

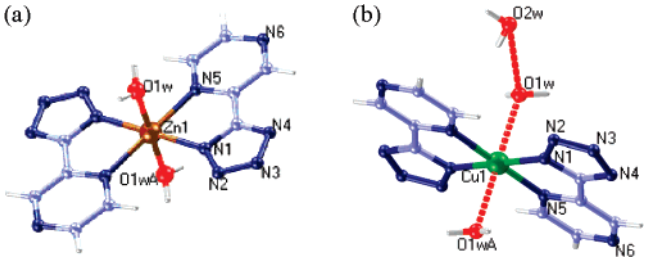

Figure 1. Mononuclear structures of complexes (a) **1** and (b) **2**, red dotted line indicates weak interaction.

ion [Cu1···O1w 2.44443(6) Å] forming the expanded octahedral geometry. Besides, there exists another guest water molecule which is responsible for the hydrogen bonding in **2** [O2w···O1w 2.858(2) Å] (Figure 1b). Each discrete $[M(pzta)_2(H_2O)_2]$ unit links four adjacent ones through hydrogen bonds [O1w···N4 2.75324(9) Å for **1** (Figure 2a); O1w···N3 2.840(3) Å, O1w···N4 2.910(3) Å for **2** (Figure 3a)] forming four-connected sublayer 4^4-nets. In complex **1**, the 4^4-subnets are further linked by other hydrogen bonds [O1w···N2 2.83161(9) Å] giving rise to a regular 3D hydrogen-bonded network (Figure 2b). Denoting $[Zn(pzta)_2(H_2O)_2]$ units as nodes and hydrogen bonds as linkers, the whole structure can be rationalized to a six-connected rhombohedral α-polonium-type ($4^{12}6^3$) network (Figure 2c).[17] Unlike the situation in **1**, the adjacent 4^4-subnets in **2** are further linked by noncoordinated water molecules (O2w in Figure 3a) through O−H···O hydrogen bonds to construct another type of 3D hydrogen-bonding framework (Figure 3b). Topologically, **2** can be rationalized to a novel binodal ($4^46^67^4$-10)(6) topological network[17] by denoting $[Cu(pzta)_2(H_2O)_2]$ as six-connected nodes and noncoordinated H_2O as interlayer-bridged two-connected nodes (Figure 3c). Here, discrete mononuclear units connect to each other through intermolecular hydrogen bonds extending to different 3D supramolecular architectures.

A fascinating structural characteristic is that there exist supramolecular water trimers linked by hydrogen bonds in the packing motif of **2**. Taking the Cu(II) atoms into account, the inorganic $[Cu(H_2O)_3]_n$ chains in complex **2**, which are formed through van der Waals forces and hydrogen bonds, run around and twist along two parallel axes forming infinite meso helices (Figure 3d). The hydrogen-bonded helices have been observed in a variety of supramolecular assemblies, but so far only a few meso helices are known.[18] Therefore, the inorganic supramolecular $[Cu(H_2O)_3]_n$ meso helix represents a particularly unusual example among tetrazole-based coordination compounds.

One-Dimensional Infinite Chain of $[Cd(pzta)_2]_n$(3). Complex **3** is a one-dimensional chain crystallizing in space group $P2_1$. As shown in Figure 4a, each Cd(II) in a slightly distorted octahedral geometry is hexacoordinated by six nitrogen atoms [Cd−N 2.290(1)−2.484(1) Å] from four pzta ligands. Two trans pzta ligands simultaneously chelated one Cd(II) center with an approximately two-faced vertical configuration [dihedral angle of two tetrazolate rings 96.56(5)°], which is different from the common trans plane in a square planar configuration.[19] The octahedron of the Cd(II) center is completed by two other nitrogen atoms from different tetrazolate rings. Each pzta ligand chelates one Cd(II) center and simultaneously bridges another one, acting as a tridentate chelating−bridging ligand. Therefore, the two adjacent Cd(II) centers are linked by two tridentate pzta ligands forming an approximately planar $Cd-N_2-Cd-N_2$ six-membered ring [Cd···Cd 4.559(2)/4.533(2) Å], and the whole structure exhibits a 1D infinite crossed-shape chain along the *a*-axis. Adjacent crossed-like chains are further packed together through intermolecular face-to-face and edge-to-face aromatic interactions (average of centroid−centroid ca. 3.6 Å), as shown in Figure 4b.

Two-Dimensional Network of $[Ag(pzta)]_n$ (4). Complex **4** consists of one pzta ligand and one Ag(I) ion in a crystallographically independent asymmetric unit, with monoclinic space group $P2_1/c$. Each Ag(I) ion features a compressed tetrahedral geometry, coordinated by four nitrogen atoms [Ag−N 2.244(3)−2.473(3)Å, N−Ag−N 72.75(9)−107.7(1)°] from three pzta ligands (Figure 5a). Each tetradentate pzta ligand bridges three Ag(I) ions, and each Ag(I) ion is linked to four other Ag(I) ions by three pzta ligands, generating a mildly undulated 2D layer sustained by coordination bonds along the *bc* plane (Figure 5a). The 2D layer structure of complex **4** can be rationalized to a (4.8^2) topological network (Figure 5b) when a pzta ligand is regarded as a three-connected node.[11c,20] A particular structural feature of **4** is that the adjacent layers are stacked to form a 3D supramolecular framework sustained by interlayer $\pi-\pi$ interaction (Figure 5c). The pzta planes of the neighboring layers are obviously parallel with each other, and the pyrazinyl···pyrazinyl rings and tetrazolate···tetrazolate rings stack in a face-to-face orientation parallel to *a*-axis [$\pi-\pi$ stacking offset distance 3.331(4) Å], implying considerably strong $\pi-\pi$ stacking interactions.

Three-Dimensional Diamondoid Framework of $[Cd_2(pzta)(OH)(SO_4)]_n$(5). The architecture of complex **5** is a three-dimensional open framework constructed by pzta ligands associated with sulfate anions. There exist three crystallographically independent Cd(II) centers in an asymmetric unit. All the Cd(II) ions are hexacoordinated. As illustrated in Figure 6a, the Cd1 center presents a highly distorted octahedron, defined by two nitrogen atoms from two different tetrazolate groups and four oxygen atoms from two sulfate anions and two hydroxyl groups [Cd1−N 2.37794(6) Å, Cd1−O 2.28246(5)−2.47937(6) Å]. Cd2 adopts a generally perfect octahedral coordination environment, similarly formed by four oxygen atoms located at an equatorial plane and two nitrogen atoms at the axial positions [Cd2−N 2.27905(5) Å, Cd2−O 2.23488(5)−2.33643(5) Å]. It is noticeable that the bond angles around the Cd2 center [N2−Cd2−N2A, O2−Cd2−O2A, O5−Cd2−O5A] are all 180°. In contrast, Cd3 exhibits distorted octahedral geometry, which is coordinated by one tetrazolate nitrogen atom and one pyrazinyl nitrogen atom from two different pzta ligands, and three oxygen atoms from three sulfate anions together with one oxygen atom from the hydroxyl groups [Cd3−N 2.35417(5)−2.52006(6) Å, Cd3−O 2.21013(5)−2.39344(6) Å]. Each pzta acts as a tetradentate bridging ligand, in which the tetrazolate group adopts a μ_3 coordinating mode and the pyrazinyl group is monodentate.

Intriguingly, the 3D structure of **5** contains pentanuclear cadmium clusters formed through Cd−S−O bonds, which consist of two sulfate anions adopting μ_5 bridging mode to link five Cd atoms (Figure 6b). Each pentanuclear cadmium cluster is connected to four adjacent clusters through two Cd2 atoms and two O4 atoms from μ_5-SO_4 units resulting in a 3D purely inorganic cationic $[Cd_2(\mu_5\text{-}SO_4)(\mu_3\text{-}OH)]^+_n$ subnet, which is further bridged by the organic anionic pzta ligands to complete the overall 3D network (Figure 6c). Regarding the pentanuclear cadmium cluster as a four-connected node, the subnet can be abstracted into a uniform four-connected 3D diamondoid network (Figure 6d). Related examples of metal−organic polymers constructed by bridging inorganic oxyacid have been reported[21] such as $[Cu(dpe)(MoO_4)]$[21b] and [Cd(bpethy)-

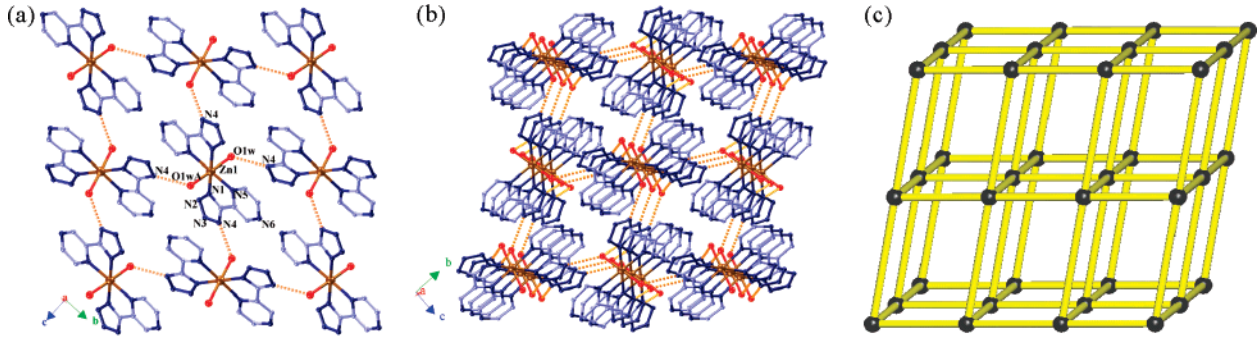

Figure 2. Complex **1**: (a) four-connected sublayer 4^4-net formed by hydrogen bonding (dotted line); (b) packing diagram showed 3D supramolecular hydrogen-bonding network (dotted line for hydrogen bond); (c) schematic representation illustrating the six-connected 3-D hydrogen-bonding net (black ball for the mononuclear complex and yellow line for hydrogen bonds). Hydrogen atoms are omitted for clarity.

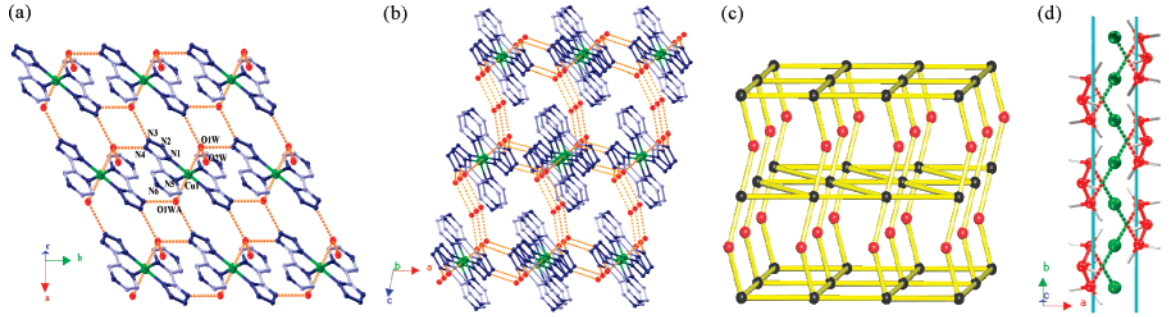

Figure 3. Complex **2**: (a) 2D 4^4-subnet layer formed by hydrogen bonding (dotted line); (b) packing diagram of 3D supramolecular hydrogen network (dotted line for hydrogen bond; hydrogen atoms are omitted for clarity); (c) schematic representation illustrating the 3D hydrogen-bonding net based on 4^4-subnets (black ball for the mononuclear complex, red ball for O_{water}, and yellow line for hydrogen-bonding); (d) schematic presentation of the meso helical $[Cu(H_2O)_3]_n$ chain (red, gray, and green balls representing O_{water}, hydrogen, and Cu, respectively).

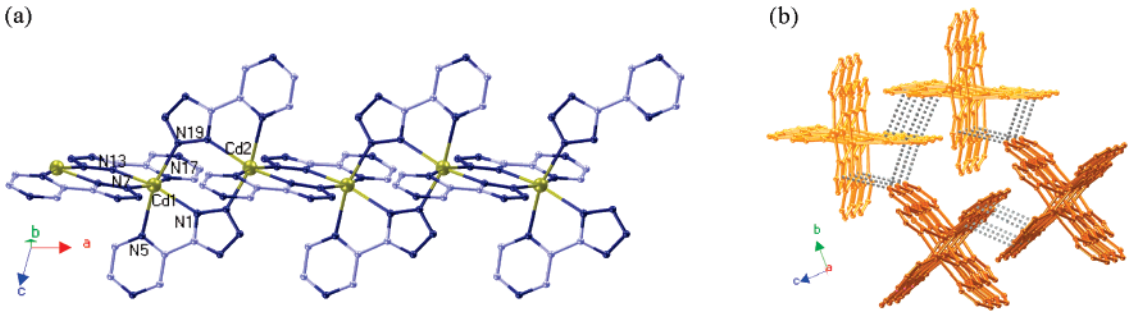

Figure 4. (a) View of the 1D chain structure of **3**. (b) Schematic representation of packing $\pi-\pi$ interaction of **3** (dotted line for $\pi-\pi$ interaction). All hydrogen atoms are omitted for clarity.

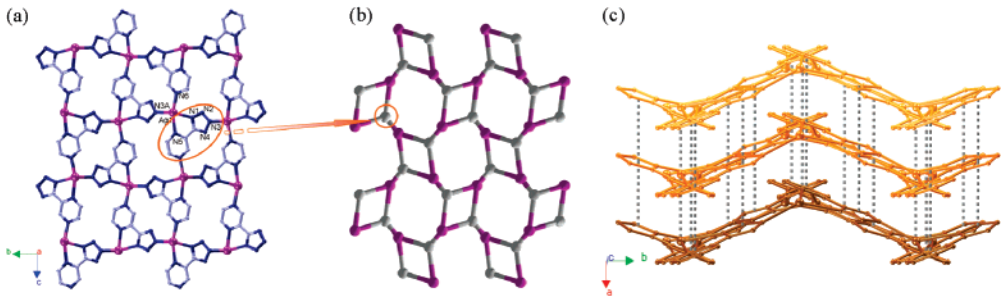

Figure 5. (a) View of the 2D layer structure of **4**. (b) 2D three-connect (4.8^2) topological network in **4**. (c) 3D packing diagram of mildly undulated layers formed through $\pi-\pi$ interactions in **4**.

$(SO_4)]$.[21d] Unlike 2D inorganic layer structures observed in those complexes, the 3D cationic inorganic $[Cd_2(\mu_5\text{-}SO_4)(\mu_3\text{-}OH)]^+_n$ diamondoid network constructed by multinuclear metal clusters in complex **5** is unprecedented, and the μ_5-SO_4 bridging mode has never been observed according to the latest CCDC database.

Coordination Modes of the Ligand. As a versatile ligand, pzta coordinates to metal ions with pyrazinyl and/or tetrazolate sites adopting bridging or chelating modes yielding a variety of coordination frameworks. In this work, successfully obtaining various dimensional metal-directed complexes enables us to

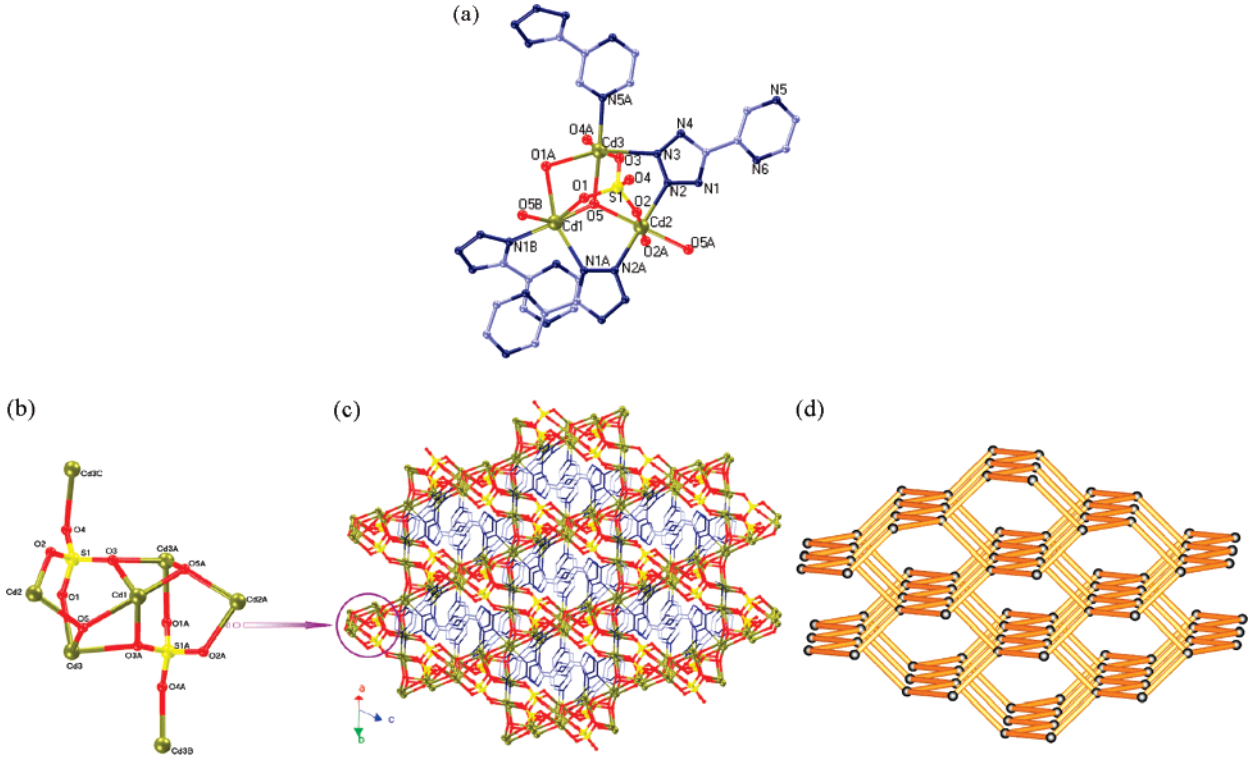

Figure 6. (a) Part of the structure of **5** showing the octahedron coordination environment of the three crystallographically independent Cd^{II} center. (b) A detailed representation of the pentanuclear cadmium cluster. (c) A representation of the overall 3D skeleton network of **5** enforced by pzta lingand (blue). (d) Topological illustration for the uniform four-connected 3D diamondoid network of **5**.

Scheme 2. Five Connection Modes of Pyrazinyl Tetrazolate Observed in Complexes 1-5

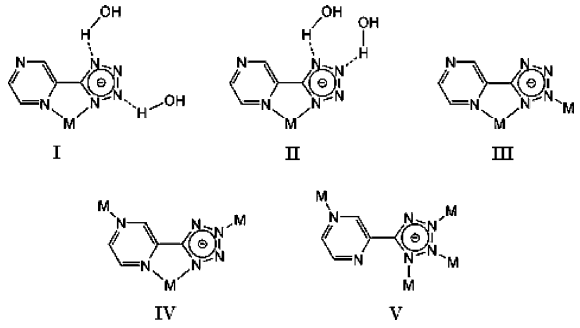

investigate the coordination modes of the pzta ligand. The in situ generated pzta ligand is readily deprotonated to form a monoanionic derivative, and is capable of being a hydrogen bonding acceptor. Scheme 2 summarizes five different coordination modes of the ligand in the complexes. In complex **1**, the pzta ligand acts as hydrogen bonding acceptor via the N2, N4 sites of the tetrazolate ring (mode I) whereas in complex **2** it acts via the N3, N4 sites (mode II). It is noticeable that complexes **1**−**4** all adopt a bidentate chelating coordination mode through the pyrazinyl N atom and tetrazolate *cis*-N atom (modes I−VI), while complex **5** adopts a tetradentate bridging mode (mode V), implying that the bridging coordinating mode is inclined to form high dimensional networks. There exist vacant N sites in the above-mentioned coordination modes; therefore, the coordination modes of the hexadentate pzta ligand should not be limited in modes I−V and be more abundant.

Photoluminescent Property. Photoluminescent measurements of the complexes were carried out in the solid state at room temperature. Complexes **1**, **3**, and **5** show strong photoluminescence upon the irradiation of ultraviolet light. Complexes **1**, **3**, and **5** are stable in air and insoluble in water or most

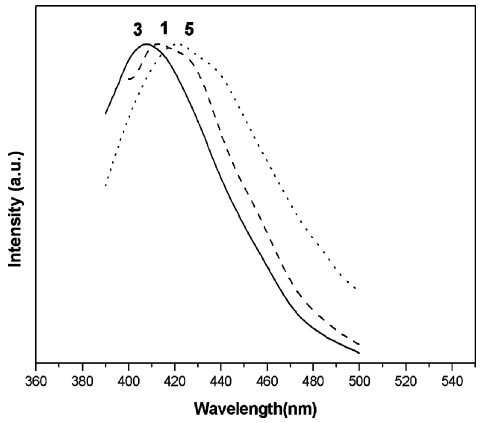

Figure 7. Emission spectra of complexes **1**, **3**, and **5** in the solid state at room temperature.

organic solvents; therefore, no additional measurement in solution could be further performed. Compounds **1**, **3**, and **5** emit with a maximum at 417, 408, and 421 nm upon the excitation at around 370 nm, respectively (Figure 7). In light of the close emission energy, the emission of the complexes is tentatively attributed to the intraligand transition of pzta modified by metal coordination. The emission in the blue region suggests that these complexes may be potential blue-light-emitting materials. Complex **2** does not exhibit detectable emission probably due to the Cu^{2+} magnetic property quenching photoluminescence. Unfortunately, the reason for no observed luminescence in **4** is not clear at this stage.

Conclusions

We have synthesized five new complexes containing in situ generated pyrazinyl tetrazolate (pzta) ligand under hydrothermal

conditions. The configurations of the series of coordination complexes exhibit an increasing dimensionality from discrete molecules to extended three-dimensional architectures. The self-assembly processes are directed by typical transition metals Zn(II), Cu(II), Cd(II), and Ag(I), adopting diverse octahedral, square-planar, or tetrahedral geometries. In the complexes, the pzta ligand is deprotonated facilely so that the strong multidentate N donors adopt chelating or bridging arrangements showing abundant coordination modes. Accordingly, the various basic units M(pzta), $M(pzta)_2$, and $M_2(pzta)$ can be alternated by using different metal ions to extend to infinite three-dimensional architectures through coordination bonds and multifarious supramolecular interactions such as hydrogen bonding and $\pi-\pi$ stacking. Our research indicates that, as a promising new type of multi-nitrogen ligand, pyrazinyl tetrazolate can be potentially utilized in constructing supramolecular structures. Moreover, this work combines various intermolecular interactions in the construction of supramolecular architectures, which contribute to increasing the knowledge of self-assembly processes and supramolecular self-organization. The blue emission of some complexes suggests that they may be potential blue-light-emitting materials.

Acknowledgment. We gratefully acknowledge the financial support provided by the National Natural Science Foundation of China (20571050 and 20271031) and the Natural Science Foundation of Guangdong Province of China (021240).

Supporting Information Available: Crystallographic data for the complexes in CIF format (CCDC 653376−653380). This material is available free of charge via the Internet at http://pubs.acs.org.

References

(1) (a) Fujita, M.; Tominaga, M.; Hori, A.; Therrien, B. *Acc. Chem. Res.* **2005**, *38*, 369. (b) Menozzi, E.; Busi, M.; Massera, C.; Ugozzoli, F.; Zuccaccia, D.; Macchioni, A.; Dalcanale, E. *J. Org. Chem.* **2006**, *71*, 2617.

(2) Fox, O. D.; Drew, M. G. B.; Beer, P. D. *Angew. Chem., Int. Ed.* **2000**, *39*, 135.

(3) Givaja, G.; Blake, A. J.; Wilson, C.; Schröder, M.; Love, J. B. *Chem. Commun*. **2005**, 4423.

(4) Furukawa, S.; Okubo, T.; Masaoka, S.; Tanaka, D.; Chang, H.-C.; Kitagawa, S. *Angew. Chem., Int. Ed*. **2005**, *44*, 2700.

(5) Du, M.; Jiang, X.-J.; Zhao, X.-J. *Inorg. Chem.* **2006**, *45*, 3998.

(6) Wang, R.; Xu, L.; Ji, J.; Shi, Q.; Li, Y.; Zhou, Z.; Hong, M.; Chan, A. S. C. *Eur. J. Inorg. Chem.* **2005**, 751.

(7) (a) Robin, A. Y.; Fromm, K. M. *Coord. Chem. Rev.* **2006**, *250*, 2127. (b) Zhang, J.-P.; Chen, X.-M. *Chem. Commun*. **2006**, 1689. (c) Katritzky, A. R.; Singh, S.; Kirichenko, K.; Smiglak, M.; Holbrey, J. D.; Reichert, W. M.; Spear, S. K.; Rogers, R. D. *Chem. Eur. J*. **2006**, *12*, 4630.

(8) (a) Rodríguez-Diéguez, A.; Colacio, E. *Chem. Commum*. **2006**, 4140. (b) Rodríguez, A.; Kivekäs, R.; Colacio, E. *Chem*. *Commum*. **2005**, 5228.

(9) For examples: (a) Wang, X.-S.; Tang, Y.-Z.; Huang, X.-F.; Qu, Z.-R.; Che, C.-M.; Chan, P. W. H.; Xiong, R.-G. *Inorg. Chem*. **2005**, *44*, 5278. (b) Ye, Q.; Li, Y.-H.; Song, Y.-M.; Huang, X.-F.; Xiong, R.-G.; Xue, Z. *Inorg. Chem.* **2005**, *44*, 3618. (c) Wang, L.-Z.; Qu, Z.-R.; Zhao, H.; Wang, X.-S.; Xiong, R.-G.; Xue, Z.-L. *Inorg. Chem.* **2003**, *42*, 3969. (d) Xiong, R.-G.; Xue, X.; Zhao, H.; You, X.-Z.; Abrahams, B. F.; Xue, Z. *Angew. Chem., Int. Ed.* **2002**, *41*, 3800. (e) Qu, Z.-R.; Zhao, H.; Wang, X.-S.; Li, Y.-H.; Song, Y.-M.; Liu, Y.-J.; Ye, Q.; Xiong, R.-G.; Abrahams, B. F.; Xue, Z.-L.; You, X.-Z. *Inorg. Chem.* **2003**, *42*, 7710. (f) Xue, X.; Wang, X.-S.; Wang, L.-Z.; Xiong, R.-G.; Abrahams, B. F.; You, X.-Z.; Xue, Z.-L.; Che, C.-M. *Inorg. Chem.* **2002**, *41*, 6544. (g) Ye, Q.; Song, Y.-M.; Wang, G.-X.; Chen, K.; Fu, D.-W.; Chan, P. W. H.; Zhu, J.-S. Huang, S. D.; Xiong, R.-G. *J. Am. Chem. Soc.* **2006**, *128*, 6554. (h) Wang, X.-S.; Tang, Y.-Z.; Xiong, R.-G. *Chin. J. Inorg. Chem.* **2005**, *21*, 1025.

(10) For examples: (a) Demko, Z. P.; Sharpless, K. B. *J. Org. Chem.* **2001**, *66*, 7945. (b) Demko, Z. P.; Sharpless, K. B. *Org. Lett.* **2001**, *3*, 4091. (c) Demko, Z. P.; Sharpless, K. B. *Angew. Chem., Int. Ed*. **2002**, *41*, 2110.

(11) (a) Wu, T.; Yi, B.-H.; Li, D. *Inorg. Chem.* **2005**, *44*, 4130. (b) Wu, T.; Chen, M.; Li, D. *Eur. J. Inorg. Chem.* **2006**, 2132. (c) Wu, T.; Zhou, R.; Li, D. *Inorg. Chem. Commun.* **2006**, *9*, 341.

(12) (a) Hou, J.-J.; Hao, Z.-M.; Zhang, X.-M. *Inorg. Chim. Acta* **2007**, *360*, 14. (b) Zhang, X.-M.; Zhao, Y.-F.; Wu, H.-S.; Batten, S. R.; Ng, S. W. *Dalton Trans.* **2006**, 3170.

(13) (a) Cantrill, S. J.; Chichak, K. S.; Peters, A. J.; Stoddart, J. F. *Acc. Chem. Res*. **2005**, *38*, 1. (b) Seidel, S. R.; Stang, P. J. *Acc. Chem. Res*. **2002**, *35*, 972. (c) Li, H.; Eddaoudi, M.; O'Keeffe, M.; Yaghi, O. M. *Nature* **1999**, *402*, 276. (d) Seo, J. S.; Whang, D.; Lee, H.; Jun, S. I.; Oh, J.; Jeon, Y. J.; Kim, K. *Nature* **2000**, *404*, 982. (e) Kim, J.; Chen, B.; Reineke, T. M.; Li, H.; Eddaoudi, M.; Moler, D. B.; O'Keeffe, M.; Yaghi, O. M. *J. Am. Chem. Soc.* **2001**, *123*, 8239. (f) Beatty, A. M. *CrystEngComm* **2001**, *51*, 1.

(14) Sheldrick, G. M. *SHELXS-97 and SHELXL-97*; Göttingen University: Göttingen, Germany, 1997.

(15) Lin, P.; Clegg, W.; Harrington, R. W.; Henderson, R. A. *Dalton Trans.* **2005**, 2388.

(16) Song, W. D., Xi, D. L. *Acta Crystallogr.* **2006**, *E62*, m2841.

(17) The topological analysis of the hydrogen bonding networks was performed using *TOPOS 4.0 Professional* software.

(18) (a) Han, L.; Hong, M. *Inorg. Chem. Commun*. **2005**, *8*, 406. (b) Becker, G.; Eschbach, B.; Mundt, O.; Seidler, N.; *Z. Anorg. Allg. Chem*. **1994**, *620*, 1381. (c) Bartlett, R. A.; Olmstead, M. M.; Power, P. P. *Inorg. Chem.* **1986**, *25*, 1243. (d) Plasseraud, L.; Maid, H.; Hampel, F.; Saalfrank, R. W. *Chem. Eur. J*. **2001**, *7*, 4007.

(19) (a) Rodríguez-Diéguez, A.; Salinas-Castillo, A.; Galli, S.; Masciocchi, N.; Gutiérrez-Zorrilla, J. M.; Vitoria, P.; Colacio, E. *Dalton Trans.* **2007**, 1821. (b) Hu, T.-L.; Li, J.-R.; Liu, C.-S.; Shi, X.-S.; Zhou, J.-N.; Bu, X.-H.; Ribas, J. *Inorg. Chem.* **2006**, *45*, 162.

(20) Zhang, J.-P.; Lin, Y.-Y.; Huang, X.-C.; Chen, X.-M. *J. Am. Chem. Soc*. **2005**, *127*, 5495.

(21) (a) Hagrman, P. J.; Hagrman, D.; Zubieta, J. *Angew. Chem., Int. Ed.* **1999**, *38*, 2638. (b) Hagrman, D.; Haushalter, R. C.; Zubieta, J. *Chem. Mater*. **1998**, *10*, 361. (c) Hagrman, D.; Warren, C. J.; Haushalter, R. C.; Seip, C.; O'Connor, C. J.; Rarig, R. S., Jr.; Johnson, K. M., III; LaDuca, R. L., Jr.; Zubieta, J. *Chem. Mater*. **1998**, *10*, 3294. (d) Carlucci, L.; Ciani, G.; Proserpio, D. M.; Rizzato, S. *CrystEngComm* **2003**, *5*, 190.

CG0702333